

See discussions, stats, and author profiles for this publication at: <https://www.researchgate.net/publication/231636513>

Matrix-Isolated van der Waals Complexes Formed between CO and Dihalogen Molecules, XY with X, Y = Cl, Br, or I

ARTICLE *in* THE JOURNAL OF PHYSICAL CHEMISTRY A · JUNE 2003

Impact Factor: 2.69 · DOI: 10.1021/jp034808s

CITATIONS

21

READS

11

2 AUTHORS:



[Rosana Romano](#)

National University of La Plata

116 PUBLICATIONS 863 CITATIONS

SEE PROFILE



[Anthony J Downs](#)

University of Oxford

258 PUBLICATIONS 5,035 CITATIONS

SEE PROFILE

Matrix-Isolated van der Waals Complexes Formed between CO and Dihalogen Molecules, XY with X, Y = Cl, Br, or I

Rosana M. Romano^{*,†,‡} and Anthony J. Downs[§]

CEQUINOR (CONICET), Departamento de Química, Facultad de Ciencias Exactas, Universidad Nacional de La Plata, 47 esq. 115, (1900) La Plata, Argentina, and Inorganic Chemistry Laboratory, University of Oxford, South Parks Road, Oxford OX1 3QR, U.K.

Received: March 28, 2003; In Final Form: May 6, 2003

Weakly bound 1:1 complexes formed between CO and a dihalogen molecule XY = Cl₂, BrCl, ICl, or IBr have been investigated by matrix-isolation experiments and density functional theory (DFT) calculations. Two families of these linear complexes exist according to whether the C or the O atom of the CO binds to the dihalogen, and with a heteronuclear dihalogen XY, this binding may occur to either of the dihalogen atoms, giving four possible isomeric forms. In addition to the $\nu(\text{CO})$ modes of the various complexes, IR measurements have identified $\nu(\text{XY})$ modes for the complexes of the type $\text{OC}\cdots\text{XY}$. The structures, vibrational properties, and binding energetics of the complexes are analyzed in light of related studies.

Introduction

How compounds containing a carbonyl function linking two nonmetal atoms respond to photolysis has attracted much attention over the years. In the past decade, for example, the La Plata group has been particularly preoccupied with carbonyl sulfonyl derivatives of the type $\text{XC}(\text{O})\text{SY}$, where the substituents X and Y may be halogen or hydrogen atoms, CH₃, or C(O)CH₃.^{1–4} When isolated in a solid inert matrix at temperatures near 10 K, these species have a relatively rich photochemistry involving conformational and isomeric changes as well as decomposition with the elimination of CO or OCS (eq 1). The studies have had as their targets not only the identifica-



tion and characterization of a variety of novel molecules so produced, including, for example, sulfur(II) halides, but also a full mechanistic interpretation of the photochemical events. Recognition that the photoisomerization of $\text{ClC}(\text{O})\text{SBr}$ to $\text{BrC}(\text{O})\text{SCl}$ hinges on the photoreversibility of reaction 1b has thus led to the first successful synthesis of $\text{BrC}(\text{O})\text{SBr}$ by broadband UV–visible photolysis of Br₂ and OCS isolated together in an Ar matrix.⁵ The photoelimination of CO (eq 1a) also being photoreversible, we have been prompted to investigate the reaction induced by photolysis of CO in the presence of various simple molecules, again under matrix conditions. The reaction with dihalogen molecules XY (where X and Y may be the same or different halogen atoms) has been shown to yield the corresponding carbonyl halides, resulting in the first sighting of the mixed halides $\text{O}=\text{ClCl}$ and $\text{O}=\text{ClBr}$.⁶ Detailed analysis

of the results of these experiments shows that photolysis is preceded by the formation of other, distinct species recognizable as being loosely bound 1:1 adducts of CO and the dihalogen and which are the focus of the present account.

van der Waals complexes such as these are important for the level of detail that is accessible through experimental and theoretical studies of their structural and dynamic properties.⁷ van der Waals complexes incorporating a CO molecule present a particular dichotomy through the possibility of forming two distinct isomeric structures according to whether the interaction engages the carbon or the oxygen atom. The existence of these two forms has been established on the evidence of both experimental and theoretical results. An extensively studied example is the complex between CO and HF.^{8–14} Both forms have been detected and characterized by their IR spectra as products of the photodissociation of matrix-isolated formyl fluoride, $\text{HC}(\text{O})\text{F}$,⁸ the consensus of experimental⁸ and ab initio¹⁵ enquiries being that $\text{OC}\cdots\text{HF}$ is slightly more stable than $\text{CO}\cdots\text{HF}$.

Complexes of the dihalogens and CO are not new. Structures and spectroscopic properties have been determined from the microwave or high-resolution rovibrational spectra of five such complexes in the gas phase, namely $\text{Cl}_2\cdots\text{CO}$,^{16,17} $\text{FCl}\cdots\text{CO}$,¹⁸ $\text{Br}_2\cdots\text{CO}$,¹⁹ $\text{ClBr}\cdots\text{CO}$,²⁰ and $\text{ClI}\cdots\text{CO}$.²¹ All are linear and feature interaction between the carbon atom of the CO and the heavier halogen in the event that the dihalogen is heteronuclear. The strength of the interaction, as measured by the intermolecular stretching force constant, varies in the order $\text{Cl}_2 < \text{Br}_2 < \text{BrCl} \leq \text{ClF} < \text{ICl}$, while the quadrupole coupling constants of the halogen atoms imply transfer of up to 0.05e of electronic charge from the bound to the terminal halogen atom.²¹ For more weakly bound isomers involving, say, coordination through the oxygen atom of CO, however, matrix isolation affords one of the few practical methods of detection and interrogation.²² Hence, we note that ab initio calculations²³ support the findings of matrix-isolation experiments identifying $\text{OC}\cdots\text{X}_2$ and $\text{CO}\cdots\text{X}_2$ (X = Cl or Br), as well as the four isomers $\text{OC}\cdots\text{BrCl}$, $\text{OC}\cdots\text{ClBr}$, $\text{CO}\cdots\text{BrCl}$, and $\text{CO}\cdots\text{ClBr}$, by the $\nu(\text{CO})$ bands appearing in their IR spectra.²⁴

* Corresponding author. Fax number: ++54 221 4259485. E-mail address: romano@quimica.unlp.edu.ar.

[†] Member of the Carrera del Investigador Científico del Consejo Nacional de Investigaciones Científicas y Técnicas, Argentina.

[‡] Universidad Nacional de La Plata.

[§] University of Oxford.

Here we describe the results of experiments in which CO has been isolated together with various dihalogens XY, where XY = Cl₂, BrCl, ICl, or IBr, in solid Ar matrixes at ~15 K. The IR spectra signal the formation of dihalogen complexes which have been identified and characterized by their $\nu(\text{CO})$ and, in some cases, by their $\nu(\text{XY})$ absorptions. The analysis is supported by ^{35,37}Cl and ^{79,81}Br isotopic shifts and also by the results of density functional theory (DFT) calculations. Hence, we seek to shed more light on the precursors to insertion reactions involving CO and XY molecules; at the same time, the data add significantly to the information base needed for a detailed mapping of the matrix photochemistry of carbonyl derivatives such as XC(O)SY.^{1–4} Similar studies of van der Waals complexes in which a dihalogen XY is engaged to either OCS or CS₂ are also in progress.⁶

Experimental and Theoretical Methods

BrCl was produced by mixing equimolar amounts of Cl₂ and Br₂ (both ex Aldrich), leading to an equilibrium mixture of BrCl, Cl₂, and Br₂.²⁵ Commercial samples of Cl₂ and Br₂ and also of ICl and IBr (again ex Aldrich) were purified by repeated trap-to-trap condensation in vacuo. CO and Ar gases (BOC, research grade) were used without further purification.

Gas mixtures were prepared by standard manometric methods. Each such mixture was deposited on a CsI window cooled to ~15 K by a Displex closed-cycle refrigerator (Air Products, model CS202) using the pulsed deposition technique.^{22,26} The IR spectrum of each matrix sample was recorded at a resolution of 0.5 cm⁻¹ and with 256 scans using a Nicolet Magna-IR 560 FTIR instrument equipped with either an MCTB or a DTGS detector (for the ranges 4000–400 cm⁻¹ or 600–250 cm⁻¹, respectively). Following deposition and IR analysis of the resulting matrix, the sample was exposed to broad-band UV–visible radiation (200 ≤ λ ≤ 800 nm) from a Spectral Energy Hg–Xe arc lamp operating at 800 W. The output from the lamp was limited by a water filter to absorb infrared radiation and so minimize any heating effects. The IR spectrum of the matrix was then recorded at different times of irradiation.

Density functional theory (DFT) calculations were performed using the Gaussian 98 program package²⁷ under the Linda parallel execution environment using two coupled personal computers. The B3LYP method was employed, with a 6-31+G* basis set for all the atoms except for iodine, to which a LANL2DZ basis set²⁸ including an effective core potential (ECP) was applied. The ECP chosen is that proposed by Hay and Wadt²⁹ which incorporates the mass velocity and Darwin relativistic effects. The LANL2DZ basis set corresponds to an effective core potential³⁰ plus a double-ζ basis for iodine atoms.

For each CO/XY system involving a heteronuclear dihalogen, the four possible complexes XY···CO, XY···OC, YX···CO, and YX···OC were investigated. Prior to the full geometry optimization of each system, a scan of the interatomic distance between the two subunits was performed. After that, and using the minimum of the potential energy curve as the starting value, a geometry optimization with simultaneous relaxation of all the geometric parameters was followed by a vibrational frequency calculation to ascertain that the optimized structure corresponded to a genuine minimum.

The binding energies were calculated using the correction proposed by Nagy et al.³¹ and expressed by eq 2:

$$\Delta E(\text{corr}) = \Delta E - \text{BSSE} + \text{GEOM} \quad (2)$$

where $\Delta E(\text{corr})$ and ΔE are the corrected and uncorrected binding energies, respectively, BSSE corresponds to the error

TABLE 1: Calculated Geometric Parameters for the Different Complexes between CO and Cl₂, BrCl, ICl, and IBr

molecular complex	r_{CO}	Δr_{CO}^a	r_{XY}	Δr_{XY}^b	$r[(\text{CO})\cdots(\text{XY})]$
OC···Cl ₂	1.1360	-1.2×10^{-3}	2.0535	$+8.0 \times 10^{-3}$	3.0501
CO···Cl ₂	1.1377	$+5 \times 10^{-4}$	2.0464	$+9 \times 10^{-4}$	3.2720
OC···ClBr	1.1365	-7×10^{-4}	2.1821	-2.5×10^{-3}	3.0340
OC···BrCl	1.1350	-2.2×10^{-3}	2.1965	$+1.19 \times 10^{-2}$	2.8872
CO···ClBr	1.1365	-7×10^{-4}	2.1821	-2.5×10^{-3}	3.0340
CO···BrCl	1.1382	-1.0×10^{-3}	2.1839	-7×10^{-4}	3.0118
OC···ClI	1.1369	-3×10^{-4}	2.4336	$+3.4 \times 10^{-3}$	3.2666
OC···ICl	1.1343	-2.9×10^{-3}	2.4522	$+2.20 \times 10^{-2}$	2.9175 ^c
CO···ClI	1.1374	$+2 \times 10^{-4}$	2.4289	-1.3×10^{-3}	3.4490
CO···ICl	1.1385	-3×10^{-4}	2.4310	$+8 \times 10^{-4}$	3.3647
OC···BrI	1.1362	-1.0×10^{-3}	2.5601	$+5.7 \times 10^{-3}$	3.1672
OC···IBr	1.1349	-2.3×10^{-3}	2.5652	$+1.08 \times 10^{-2}$	3.0661
CO···BrI	1.1377	$+5 \times 10^{-4}$	2.5538	-6×10^{-4}	3.3153
CO···IBr	1.1383	-1.1×10^{-3}	2.5539	-5×10^{-4}	3.4438

^a $\Delta r_{\text{CO}} = r_{\text{CO,complex}} - r_{\text{CO,free}}$. ^b $\Delta r_{\text{XY}} = r_{\text{XY,complex}} - r_{\text{XY,free}}$. ^c Experimental intermolecular distance = 3.011 Å.²¹

due to the basis set superposition, and the term GEOM takes into account the geometry differences between free CO and XY monomers and each of the subunits as they occur in the complex dimer. These terms can be calculated through eqs 3–5:

$$\Delta E = E(\text{AB}) - E^{m,m}(\text{A}) - E^{m,m}(\text{B}) \quad (3)$$

$$\text{BSSE}_{(d,d-m)} = E^{d,d}(\text{A}) - E^{d,m}(\text{A}) + E^{d,d}(\text{B}) - E^{d,m}(\text{B}) \quad (4)$$

$$\text{GEOM}_{(d,m-m,m)} = E^{d,m}(\text{A}) - E^{m,m}(\text{A}) + E^{d,m}(\text{B}) - E^{m,m}(\text{B}) \quad (5)$$

where the superscripts m and d refer to the monomers and dimer, respectively. The first superscript refers to the geometry of the species, and the second one refers to the basis set used to calculate the energy at a geometry defined by the first superscript. The terms BSSE have been calculated by applying the counterpoise procedure developed by Boys and Benardi.³²

Results and Discussion

(i) Theoretical Calculations. (a) *Equilibrium Geometries.* In keeping with the results of earlier calculations,²³ the only 1:1 complexes to be investigated in detail were those with collinear CO and XY fragments. Our calculations thus confirmed that Cl₂ forms two possible complexes, each corresponding to a potential energy minimum, viz. OC···Cl₂ and CO···Cl₂. With BrCl, ICl, or IBr, however, four possible complexes can be identified, namely the linear species OC···XY, CO···XY, OC···YX, and CO···YX, each also corresponding to a true minimum in the potential energy surface with no imaginary vibrational frequencies. The calculated geometric parameters for the optimized structures are given in Table 1. Where comparison can be made, there is satisfactory agreement with the results of the earlier (ab initio) calculations and also with the dimensions determined experimentally.^{16,17,20,21} For example, the calculated (r_e) I···C distance of 2.92 Å for OC···ICl compares with the experimentally determined one (r_0) of 3.011(1) Å.²¹ The I···O distance in CO···ICl is calculated to be 3.36 Å, whereas the Cl···C and Cl···O distances in OC···ClI and CO···ClI are 3.27 and 3.45 Å, respectively. The I···C distance in OC···IBr is predicted to be 3.07 Å, that is, 0.15 Å longer than that in OC···ICl.

(b) *Vibrational Properties.* The IR spectrum anticipated for each of the complexes is dominated by the $\nu(\text{CO})$ and $\nu(\text{XY})$ modes. All the other fundamentals are characterized by wave-

TABLE 2: Calculated Wavenumbers (in cm^{-1}) for the Different Complexes between CO and Cl_2 , BrCl , ICl , and IBr

molecular complex	$\nu(\text{CO})$	$\Delta\nu(\text{CO})^a$	$\nu(\text{XY})$	$\Delta\nu(\text{XY})^b$
$\text{OC}\cdots\text{Cl}_2$	2213.9	+11.5	498.7	-15.0
$\text{CO}\cdots\text{Cl}_2$	2198.8	-3.6	512.8	-0.9
$\text{OC}\cdots\text{ClBr}$	2210.6	+8.2	429.4	-2.9
$\text{OC}\cdots\text{BrCl}$	2221.1	+18.7	418.2	-14.1
$\text{CO}\cdots\text{ClBr}$	2199.5	-2.9	437.6	+5.3
$\text{CO}\cdots\text{BrCl}$	2193.9	-8.5	433.5	+1.2
$\text{OC}\cdots\text{ClI}$	2206.5	+4.1	334.2	-4.1
$\text{OC}\cdots\text{ICl}$	2225.3	+22.9	320.9	-17.4
$\text{CO}\cdots\text{ClI}$	2202.0	-0.4	339.5	+1.2
$\text{CO}\cdots\text{ICl}$	2193.2	-9.2	336.3	-2.0
$\text{OC}\cdots\text{BrI}$	2213.6	+11.2	244.0	-4.3
$\text{OC}\cdots\text{IBr}$	2221.3	+18.9	239.7	-8.6
$\text{CO}\cdots\text{BrI}$	2199.6	-2.8	249.0	+0.7
$\text{CO}\cdots\text{IBr}$	2195.3	-7.1	247.7	-0.6

^a $\Delta\nu(\text{CO}) = \nu(\text{CO})_{\text{complex}} - \nu(\text{CO})_{\text{free}}$. ^b $\Delta\nu(\text{XY}) = \nu(\text{XY})_{\text{complex}} - \nu(\text{XY})_{\text{free}}$.

numbers well below the low-energy threshold (250 cm^{-1}) of the present IR measurements and, in any case, by low intensities. For a given unsymmetrical dihalogen XY, the different complexes may be distinguished, it appears, on the basis of their $\nu(\text{CO})$ and $\nu(\text{XY})$ wavenumbers (see Table 2). Thus, $\text{OC}\cdots\text{XY}$ shows a blue shift in $\nu(\text{CO})$ and a red shift in $\nu(\text{XY})$ compared with free CO and XY, respectively. On the other hand, $\text{CO}\cdots\text{XY}$ shows not a blue but a red shift in $\nu(\text{CO})$ and a reduced red shift in $\nu(\text{XY})$. Reversing a heteronuclear XY molecule so that coordination occurs to the less polarizable halogen atom rather than the more polarizable one produces the same general pattern but with much smaller shifts in $\nu(\text{CO})$ and $\nu(\text{XY})$, suggesting that it may well be difficult in practice to identify the complex in the presence of free XY and free CO.

(c) *Binding Energies.* The binding energies, ΔE , calculated for the different complexes on the basis of eq 3 are presented in Table 3, which also lists the two terms that contribute to the corrected energy, viz. BSSE (eq 4) and GEOM (eq 5). The complexes having the highest binding energies are, as might be expected, $\text{OC}\cdots\text{ICl}$ and $\text{OC}\cdots\text{IBr}$ with stabilization energies with respect to the corresponding isolated monomers of 2.55 and 1.64 kcal mol^{-1} , respectively.

(d) *NBO Analysis.* Natural bond Orbital (NBO) analysis is now accepted as a very useful guide to the bonding properties of van der Waals complexes as interpreted in terms of "donor-acceptor" interactions.³³ NBO analysis of all the dihalogen complexes of CO for which calculations have been performed predicts charge transfer from the CO to the dihalogen. The

amount of charge transferred (q) depends on the complex (see Table 3), being greatest for the $\text{OC}\cdots\text{ICl}$ and $\text{OC}\cdots\text{IBr}$ complexes, for which it reaches values of ~ 0.06 and $0.04e$, respectively. Experimental estimates based on the nuclear quadrupole coupling constants of the halogen atoms give a value of $0.025(2)e$ for $\text{OC}\cdots\text{ICl}$.²¹ The largest contribution to the stabilization energy arises from the interaction of the lone pair of the C (for the $\text{OC}\cdots\text{XY}$ complexes) or O atom (for the $\text{CO}\cdots\text{XY}$ complexes) with the unfilled σ antibonding orbital of the dihalogen molecule. This energy lowering could be expressed by the following second-order equations:

$$\Delta E_{\text{no}^*}(\text{OC}\cdots\text{XY}) = -2 \frac{\langle n_{\text{C}} | \hat{F} | \sigma_{\text{XY}}^* \rangle^2}{\epsilon_{\sigma_{\text{XY}}^*} - \epsilon_{n_{\text{C}}}} \quad (6)$$

$$\Delta E_{\text{no}^*}(\text{CO}\cdots\text{XY}) = -2 \frac{\langle n_{\text{O}} | \hat{F} | \sigma_{\text{XY}}^* \rangle^2}{\epsilon_{\sigma_{\text{XY}}^*} - \epsilon_{n_{\text{O}}}} \quad (7)$$

in which F is the Fock operator and ϵ 's are the orbital energies. The calculated values for the energy lowering due to this interaction, also included in Table 3, reach a maximum in $\text{OC}\cdots\text{ICl}$, with a stabilization of $13.79\text{ kcal mol}^{-1}$.

(ii) *Experimental Findings.* (a) *$\text{Cl}_2/\text{CO}/\text{Ar}$ Mixtures.* The structural and spectroscopic properties of the weakly bonded complexes formed between CO and Cl_2 molecules have been the subject of previous experimental and theoretical studies.^{16,17,23,24} The complex $\text{OC}\cdots\text{Cl}_2$ is linear with a $\text{Cl}\cdots\text{C}$ distance of 3.134 \AA .²¹ Only the $\nu(\text{CO})$ spectral region has been investigated previously, revealing a 6.28 cm^{-1} blue shift relative to the case of the free CO molecule. These findings are supported by ab initio studies,²³ which find minima for two linear structures, $\text{CO}\cdots\text{Cl}_2$ and $\text{OC}\cdots\text{Cl}_2$, with the latter being slightly more stable than the former; in addition, high-energy minima are found for two nonlinear structures, one T-shaped and the other with an essentially parallel array of the two molecules. A more recent study²⁴ has involved matrix isolation of the $\text{OC}\cdots\text{Cl}_2$ complex following codeposition of Ar or N_2 samples doped with Cl_2 and CO at concentrations varying from 1/500 to 1/200 for Cl_2 and from 1/10000 to 1/1000 for CO. The $\text{CO}\cdots\text{Cl}_2$ complex was subsequently recognized after irradiation of the matrix. Both complexes were identified only by their $\nu(\text{CO})$ modes in the IR spectrum; no absorption due to the perturbed Cl_2 molecule was observed.

In the present study, a mixture of 0.5 Torr of Cl_2 , 1 Torr of CO, and 200 Torr of Ar was deposited on the cooled CsI window. The strongest feature of the IR spectrum, measured immediately after deposition, was observed at 2138.2 cm^{-1} ,

TABLE 3: Calculated Uncorrected and Corrected Binding Energies ΔE , BSSE and GEOM Corrections, Net Charge q Transferred, and Orbital Stabilization for the Different Complexes between CO and Cl_2 , BrCl , ICl , and IBr

molecular complex	$\Delta E (\text{kcal}\cdot\text{mol}^{-1})$	$\Delta E(\text{corr}) (\text{kcal}\cdot\text{mol}^{-1})$	BSSE ($\text{kcal}\cdot\text{mol}^{-1}$)	GEOM ($\text{kcal}\cdot\text{mol}^{-1}$)	$q (e)$	$\Delta E_{\text{no}^*} (\text{kcal}\cdot\text{mol}^{-1})$
$\text{OC}\cdots\text{Cl}_2$	+1.04	+0.77	+0.29	-0.02	0.0194	-2.66
$\text{CO}\cdots\text{Cl}_2$	+0.28	+0.16	+0.12	-6×10^{-4}	0.0015	-0.16
$\text{OC}\cdots\text{ClBr}$	+3.44	+0.35	+3.09	-4×10^{-3}	0.0185	-2.11
$\text{OC}\cdots\text{BrCl}$	+4.44	+1.81	+2.64	-0.01	0.0431	-6.42
$\text{CO}\cdots\text{ClBr}$	+2.43	-0.06	+2.50	-7×10^{-3}	0.0024	-0.47
$\text{CO}\cdots\text{BrCl}$	+2.56	+0.25	+2.31	-4×10^{-3}	0.0045	-0.92
$\text{OC}\cdots\text{ClI}$	-0.81	+0.09	-0.90	-2×10^{-3}	0.0116	-1.18
$\text{OC}\cdots\text{ICl}$	+1.51	+2.55	-0.96	-0.08	0.0630	-13.79
$\text{CO}\cdots\text{ClI}$	-1.13	-0.07	-1.06	-4×10^{-4}	0.0004	-0.10
$\text{CO}\cdots\text{ICl}$	-0.68	+0.52	-1.20	-3×10^{-3}	0.0032	-0.98
$\text{OC}\cdots\text{BrI}$	+0.12	+0.56	-0.43	-3×10^{-3}	0.0013	-0.36
$\text{OC}\cdots\text{IBr}$	+0.82	+1.64	-0.80	+0.02	0.0442	-8.74
$\text{CO}\cdots\text{BrI}$	-0.63	+0.05	-0.68	-7×10^{-4}	0.0013	-0.36
$\text{CO}\cdots\text{IBr}$	-0.73	+0.38	-1.11	-2×10^{-3}	0.0022	-0.74

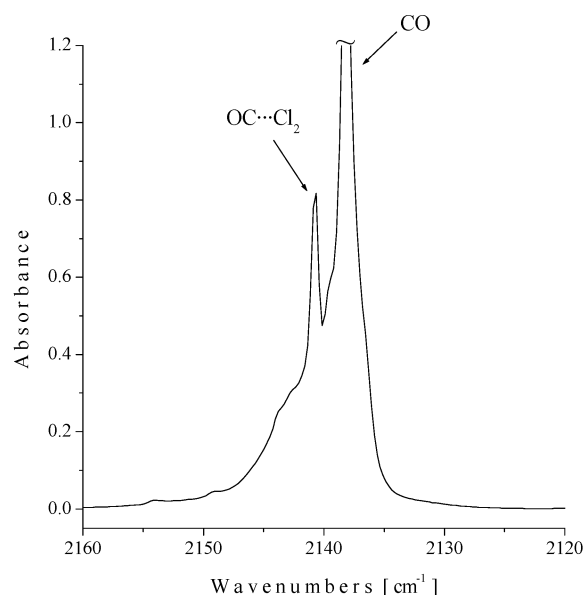


Figure 1. FTIR spectrum in the $\nu(\text{CO})$ spectral region for an Ar matrix formed by codeposition of a gaseous mixture of Cl_2 , CO, and Ar (0.5:1:200).

corresponding to the $\nu(\text{CO})$ mode of the free, uncomplexed CO molecule.³⁴ As shown in Figure 1, however, there was an additional band at 2140.7 cm^{-1} observed only when Cl_2 was present. This was shifted by $+2.5 \text{ cm}^{-1}$ with respect to the case of free CO, in close agreement with the $+2.1 \text{ cm}^{-1}$ shift reported previously for the complex $\text{OC}\cdots\text{Cl}_2$ isolated in an Ar matrix²⁴ but considerably smaller than the shift of $+6.29 \text{ cm}^{-1}$ determined for the gaseous complex.²¹ The relative intensities of the two bands were in accordance with the proportions of the two components in the mixture. This experiment, performed under conditions different from those in the previous study,²⁴ provides validation of the present methods of forming and interrogating the complex $\text{OC}\cdots\text{Cl}_2$.

In addition to the bands assigned to free and perturbed CO depicted in Figure 1, a weak triplet could also be discerned at 545.0 , 537.6 , and 530.3 cm^{-1} (with relative intensities approximating to 9:6:1), as shown in Figure 2. This set of bands is most plausibly assigned to the perturbed Cl_2 molecule in the $\text{OC}\cdots\text{Cl}_2$ complex. The corresponding values for free Cl_2 isolated in a solid Ar matrix, determined by laser-induced fluorescence and Raman spectroscopy,³⁵ are reported to be 549.1 , 541.8 , and 534.3 cm^{-1} for $^{35}\text{Cl}_2$, $^{35}\text{Cl}^{37}\text{Cl}$, and $^{37}\text{Cl}_2$, respectively. The $\nu(\text{ClCl})$ mode, inactive in the free molecule, becomes weakly active in IR absorption in the complex, where the symmetry is reduced to $C_{\infty v}$, and appears to suffer a red shift of 4.1 cm^{-1} . In none of the previous studies has this feature been reported. Included in Table 4 for comparison are the results of the DFT (B3LYP/6-31+G*) calculations, which anticipate faithfully the sense, if not the exact magnitude, of the $\nu(\text{CO})$ and $\nu(\text{ClCl})$ shifts induced by complexation. As noted previously,²⁴ such shifts change markedly with the switch from the gas to the matrix phase and also from one matrix to another, reflecting presumably the susceptibility of the weakly bound complex to constraint and polarization under the action of the matrix cage.

(b) $\text{Cl}_2/\text{Br}_2/\text{CO}/\text{Ar}$ Mixtures. A mixture of gaseous chlorine and bromine gives rise to an equilibrium between these two species and the interhalogen BrCl .²⁵ The complexes formed between the components of this equilibrated mixture and CO in an Ar matrix have been described previously.²⁴ The results

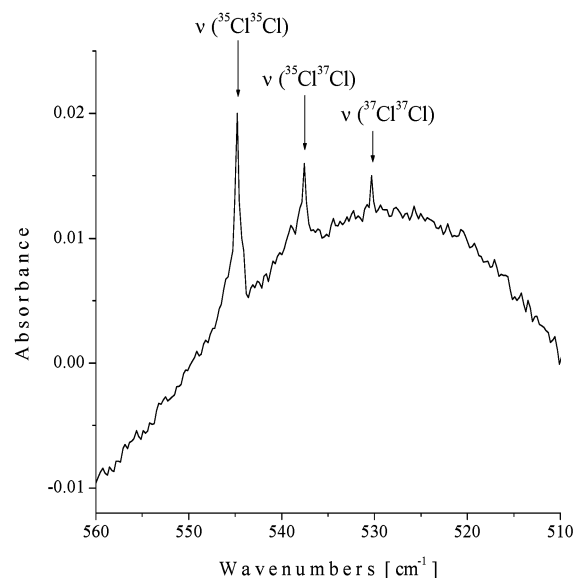


Figure 2. FTIR spectrum in the $\nu(\text{Cl}_2)$ spectral region for an Ar matrix formed by codeposition of a gaseous mixture of Cl_2 , CO, and Ar (0.5:1:200).

TABLE 4: Comparison of the Experimental and Calculated Wavenumbers (in cm^{-1}) for the $\text{OC}\cdots\text{Cl}_2$ Complex

mode	experimental (Ar matrix)		B3LYP/6-31+G*	
	$\nu \text{ (cm}^{-1}\text{)}$	$\Delta\nu \text{ (cm}^{-1}\text{)}$	$\nu \text{ (cm}^{-1}\text{)}$	$\Delta\nu \text{ (cm}^{-1}\text{)}$
$\nu(\text{CO})$	2140.7	+2.5 (+2.1 ^a)	2213.9	+11.5
$\nu(\text{Cl}_2) \text{ } ^{35}\text{Cl}-^{35}\text{Cl}\cdots\text{CO}$	545.0	-4.1	498.7	-15.0
$\nu(\text{Cl}_2) \text{ } ^{35}\text{Cl}-^{37}\text{Cl}\cdots\text{CO}$	537.6	-4.2	492.0	-14.8
$\nu(\text{Cl}_2) \text{ } ^{37}\text{Cl}-^{35}\text{Cl}\cdots\text{CO}$			491.8	-15.0
$\nu(\text{Cl}_2) \text{ } ^{37}\text{Cl}-^{37}\text{Cl}\cdots\text{CO}$	530.3	-4.0	485.0	-14.7

^a Reference 19.

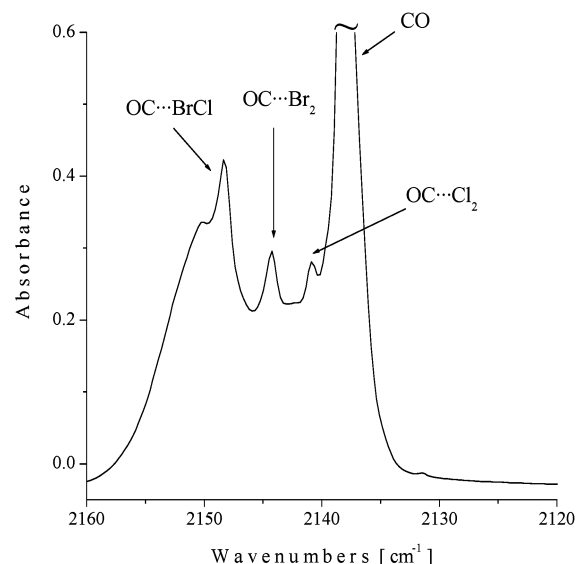


Figure 3. FTIR spectrum in the $\nu(\text{CO})$ spectral region for an Ar matrix formed by codeposition of a gaseous mixture initially made of Cl_2 , Br_2 , CO, and Ar (2:2:1:200).

of our experiments involving codeposition of a mixture initially made up with Cl_2 , Br_2 , CO, and Ar in the proportions 2:2:1:200 are completely consistent with those reported earlier.²⁴ Figure 3 illustrates the IR spectrum of the matrix in the $\nu(\text{CO})$ region. Absorption maxima at 2148.3 , 2144.3 , and 2140.8 cm^{-1} can be assigned to the species $\text{OC}\cdots\text{BrCl}$, $\text{OC}\cdots\text{Br}_2$, and

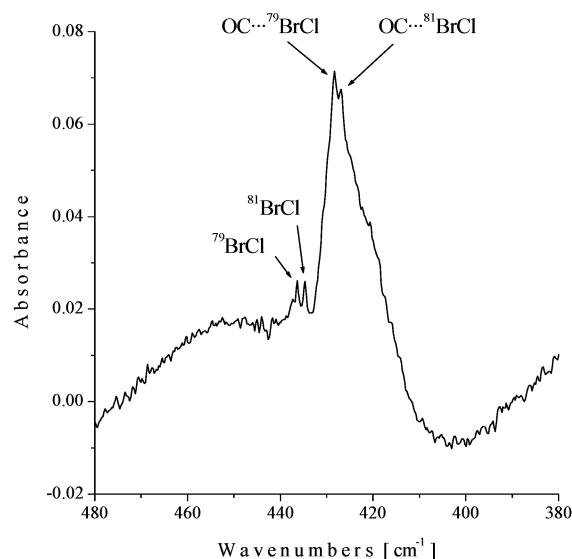


Figure 4. FTIR spectrum in the $\nu(\text{BrCl})$ spectral region for an Ar matrix formed by codeposition of a gaseous mixture initially made of Cl_2 , Br_2 , CO, and Ar (2:2:1:200).

TABLE 5: Comparison of the Experimental and Calculated Wavenumbers (in cm^{-1}) for the $\text{OC}\cdots\text{BrCl}$ Complex

mode	experimental (Ar matrix)		B3LYP/6-31+G*	
	ν (cm^{-1})	$\Delta\nu$ (cm^{-1})	ν (cm^{-1})	$\Delta\nu$ (cm^{-1})
$\nu(\text{CO})$	2148.3	+10.2 (+9.5 ^a)	2221.1	+18.7
$\nu(\text{BrCl}) \text{ Cl}-^{79}\text{Br}\cdots\text{CO}$	428.4	-8.0	418.2	-14.1
$\nu(\text{BrCl}) \text{ Cl}-^{81}\text{Br}\cdots\text{CO}$	427.0	-7.8	416.7	-14.0

^a Reference 24.

$\text{OC}\cdots\text{Cl}_2$, respectively, in close conformity with the earlier values of 2147.9, 2143.9, and 2140.6 cm^{-1} . The remaining complex in which the CO interacts through the carbon atom, that is, $\text{OC}\cdots\text{ClBr}$, is reported to absorb at 2138.0 cm^{-1} , but this was obscured in our case by the band due to free CO at 2138.2 cm^{-1} .³⁴

The $\text{OC}\cdots\text{BrCl}$ complex can also be identified by a red shift in the absorptions associated with the $\nu(\text{BrCl})$ mode, as shown in Figure 4. Bands at 436.3 and 434.8 cm^{-1} have been reported³ for the species $^{79}\text{BrCl}$ and $^{81}\text{BrCl}$ as formed by photolysis of ClC(O)SBr isolated in an Ar matrix. Attempts to record the IR spectrum of BrCl isolated in an inert gas matrix have resulted in rather complicated spectra that may be interpreted in terms of different molecular aggregates of the molecules BrCl , Cl_2 , and Br_2 .⁶ Comparison with our earlier studies³ suggests that the weak absorptions observed at 436.4 and 434.8 cm^{-1} in the spectrum of a matrix that also included CO should be assigned to the uncomplexed BrCl molecules. The much stronger doublet appearing at 428.4 and 427.0 cm^{-1} , which is not present in the spectrum of a matrix otherwise similar but containing no CO, is attributable to the isotopomers $\text{OC}\cdots^{79}\text{BrCl}$ and $\text{OC}\cdots^{81}\text{BrCl}$, respectively. As can be seen in Figure 4, isotopic splitting of the $\nu(\text{BrCl})$ mode associated with the $^{35/37}\text{Cl}$ isotopes overlaps with the modes due to different molecular aggregates of the molecules BrCl , Cl_2 , and Br_2 . The comparison between the experimental and DFT wavenumbers is presented in Table 5.

(c) *ICl/CO/Ar Mixtures.* Different gaseous mixtures of ICl, CO, and Ar were codeposited on the cooled CsI window, and the matrix was subsequently irradiated with broad-band UV–visible light ($200 \leq \lambda \leq 800$ nm). In addition to the band corresponding to free CO, new features appeared at 2157.0, 2154.0, 2145.6, 2144.2, and 2128.4 cm^{-1} in the $\nu(\text{CO})$ region

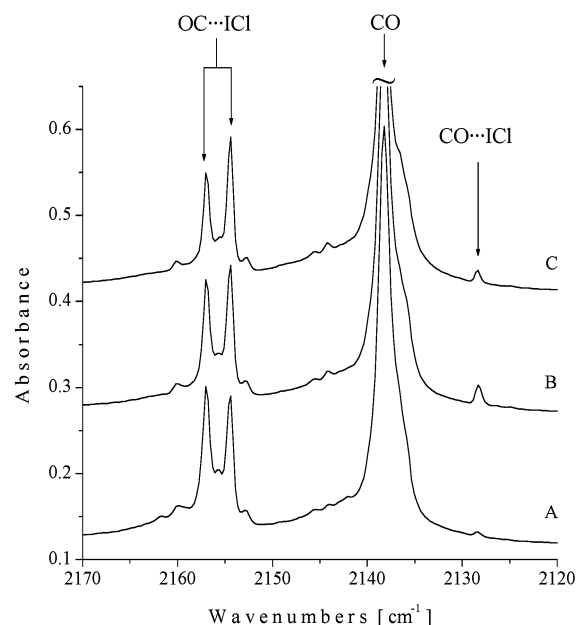


Figure 5. FTIR spectra in the $\nu(\text{CO})$ spectral region for an Ar matrix formed by codeposition of a gaseous mixture of ICl, CO, and Ar (0.5:1:200): (A) before photolysis; (B) after 15 min of photolysis; (C) after 1 h of photolysis with broad-band UV–visible light ($200 \leq \lambda \leq 800$ nm).

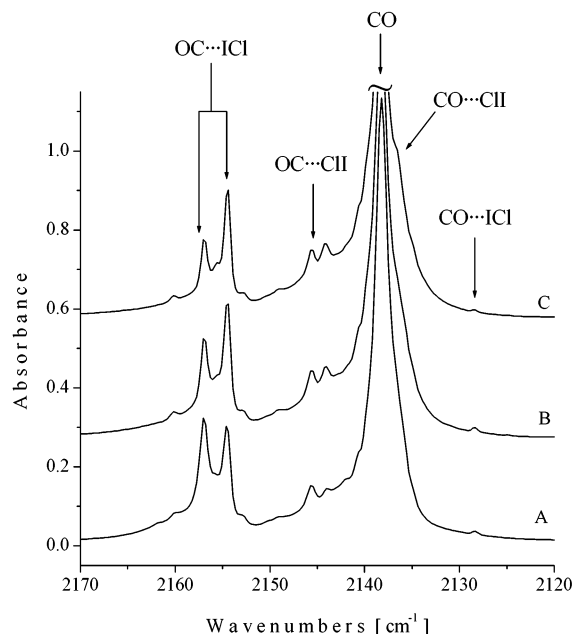


Figure 6. FTIR spectra in the $\nu(\text{CO})$ spectral region for an Ar matrix formed by codeposition of a gaseous mixture of ICl, CO, and Ar (1:1:200): (A) before photolysis; (B) after 30 min of photolysis; (C) after 2 h of photolysis with broad-band UV–visible light ($200 \leq \lambda \leq 800$ nm).

of the IR spectrum of the matrix immediately after deposition. Figure 5A shows the IR spectrum of such a matrix with ICl, CO, and Ar in the proportions 0.5:1:200, while Figure 6A shows the corresponding spectrum for a 1:1:200 mixture.

Taking into account the ambidentate character of the CO and ICl molecules, we envisage four possible complexes that may be formed in these experiments, namely $\text{OC}\cdots\text{ICl}$, $\text{OC}\cdots\text{CII}$, $\text{CO}\cdots\text{ICl}$, and $\text{CO}\cdots\text{CII}$. The most intense absorptions in both experiments are those occurring at 2157.0/2154.0 cm^{-1} that we assign to the $\nu(\text{CO})$ fundamental of the $\text{OC}\cdots\text{ICl}$ complex occupying two different matrix sites, partly on the basis of

TABLE 6: Comparison of the Experimental and Calculated Wavenumbers (in cm^{-1}) for the Different Possible Complexes Formed between CO and ICl

complex	mode	experimental (Ar matrix)		B3LYP/6-31+G*	
		ν (cm^{-1})	$\Delta\nu$ (cm^{-1})	ν (cm^{-1})	$\Delta\nu$ (cm^{-1})
OC...ICl	$\nu(\text{CO})$	{ 2157.0 2154.0	{ +18.8 +15.8	2225.3	+22.9
	$\nu(\text{I}^{35}\text{Cl})$	369.6	-6.4	320.9	-17.4
	$\nu(\text{I}^{37}\text{Cl})$	361.7	-6.4	313.9	-17.1
OC...CII	$\nu(\text{CO})$	{ 2145.6 2144.2	{ +7.4 +6.0	2206.5	+4.1
	$\nu(\text{I}^{35}\text{Cl})$			334.2	-4.1
	$\nu(\text{I}^{37}\text{Cl})$			327.1	-3.9
CO...ICl	$\nu(\text{CO})$	2128.4	-9.8	2193.2	-9.2
	$\nu(\text{I}^{35}\text{Cl})$			336.3	-2.0
	$\nu(\text{I}^{37}\text{Cl})$			329.1	-1.9
CO...CII	$\nu(\text{CO})$	2136.5	-1.7	2202.0	-0.4
	$\nu(\text{I}^{35}\text{Cl})$			339.5	+1.2
	$\nu(\text{I}^{37}\text{Cl})$			332.2	+1.2

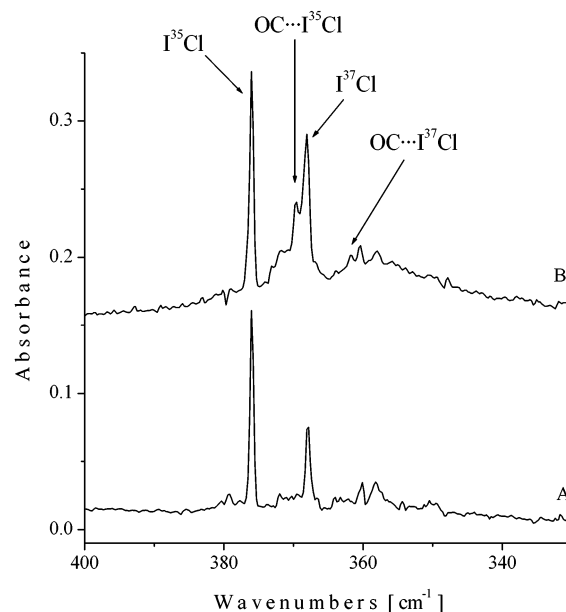
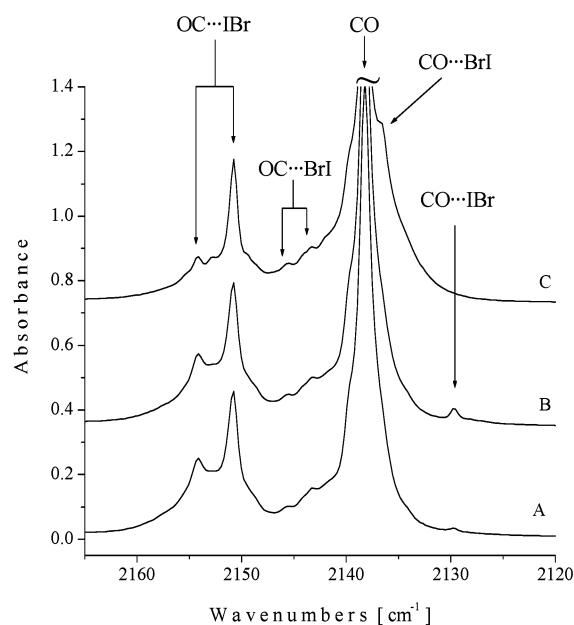
predicted spectrum (see Table 2) and partly in light of the relative stabilities predicted by the DFT calculations (see Table 3). With respect to the case of free CO, a blue shift of +18.8/15.8 cm^{-1} is thus indicated for this complex.

The features at 2145.6/2144.2 cm^{-1} , blue-shifted by 7.4/6.0 cm^{-1} with respect to the case of free CO, grow as the proportion of the dihalogen molecule in the mixture increases. There is also a slight intensification of these bands on exposure of the matrix to broad-band UV–visible radiation. Drawing on the predictions of the DFT calculations, we attribute these absorptions to the OC...CII complex, also occupying two different matrix sites.

The band at 2128.4 cm^{-1} , with a 9.8 cm^{-1} red shift with respect to the case of free CO, first grows and then decays as a function of irradiation time. Accordingly, it may be assigned to a complex in which CO coordinates through the O atom, namely CO...ICl. A shoulder on the absorption due to free CO appearing at 2136.5 cm^{-1} is then the obvious candidate for the $\nu(\text{CO})$ fundamental of the fourth complex CO...CII. Table 6 compiles the experimental and calculated wavenumbers of the four different linear complexes formed between CO and ICl.

The absorption corresponding to the $\nu(\text{ICl})$ mode near 370 cm^{-1} also showed a shift on complexation. Figure 7A illustrates the IR spectrum of an Ar matrix doped with ICl. The doublet appearing at 376.0/368.0 cm^{-1} corresponds to the isotopomers I^{35}Cl and I^{37}Cl , respectively, in agreement with the results of earlier experiments.³⁶ When ICl was mixed with CO in an Ar matrix, a new IR band appeared at 369.6 cm^{-1} , that is, 6.4 cm^{-1} red-shifted with respect to $\nu(\text{I}^{35}\text{Cl})$ of free ICl (see Figure 7B). This band is most plausibly assigned to $\nu(\text{ICl})$ of the OC...ICl complex, since it tracked the most intense feature in the $\nu(\text{CO})$ region, viz. the doublet at 2157.0/2154.0 cm^{-1} associated with what is undoubtedly the main product. All of the other complexes were formed in substantially lower concentrations and are expected to feature $\nu(\text{ICl})$ fundamentals at wavenumbers much closer to those of free ICl (see Table 6), making them that much more difficult to detect.

(d) *IBr/CO/Ar Mixtures.* Figure 8A illustrates the $\nu(\text{CO})$ region of the IR spectrum of a matrix formed by codeposition of a gaseous mixture of 0.5 Torr of IBr, 1 Torr of CO, and 200 Torr of Ar. The matrix was subsequently irradiated with broad-band UV–visible light, first for 15 min and then for 1 h. The corresponding spectra are shown as traces 8B and 8C, respectively. No useful absorption could be associated with the $\nu(\text{IBr})$ mode of either free IBr or any complex with CO; this would be expected to occur near 270 cm^{-1} , close to the low-energy cutoff of the present measurements.

**Figure 7.** FTIR spectra in the $\nu(\text{ICl})$ spectral region for an Ar matrix formed by codeposition of a gaseous mixture of (A) ICl and Ar (1:200) and (B) ICl, CO, and Ar (1:1:200).**Figure 8.** FTIR spectra of an Ar matrix formed by codeposition of a gaseous mixture of IBr, CO, and Ar (0.5:1:200): (A) before photolysis; (B) after 15 min of photolysis; (C) after 1 h of photolysis with broad-band UV–visible light ($200 \leq \lambda \leq 800$ nm).

The most prominent of the new features to be observed when IBr was present were those at 2154.1 and 2150.8 cm^{-1} , which may be associated with the molecular complex OC...IBr occupying two different matrix sites. This is the most stable of the four possible linear complexes according to our theoretical predictions (see Table 3), showing a substantial blue shift with respect to the case of free CO (+15.9/12.6 cm^{-1}). A much weaker pair of bands at 2145.5/2143.2 cm^{-1} , blue-shifted by +7.3/5.0 cm^{-1} , belongs presumably to the second carbon-bound isomer OC...BrI, whereas two other weak bands at 2129.7 and 2136.5 cm^{-1} , which were observed to develop on photolysis, originate in CO...IBr and CO...BrI, respectively. As indicated in Table 7, these results are wholly consistent with the properties predicted by the DFT calculations.

TABLE 7: Comparison of the Experimental and Calculated Wavenumbers (in cm^{-1}) for the $\nu(\text{CO})$ Mode of the Different Possible Complexes Formed between CO and IBr

complex	experimental (Ar matrix)		B3LYP/6-31+G*	
	ν (cm^{-1})	$\Delta\nu$ (cm^{-1})	ν (cm^{-1})	$\Delta\nu$ (cm^{-1})
OC \cdots IBr	2154.1	+15.9	2221.3	+18.9
	2150.8	+12.6		
OC \cdots BrI	2145.5	+7.3	2213.2	+10.8
	2143.2	+5.0		
CO \cdots IBr	2129.7	-8.5	2195.3	-7.1
CO \cdots BrI	2136.5	-1.7	2199.6	-2.8

Conclusions

DFT calculations confirm the existence of two families of weakly bound, linear dihalogen-CO complexes with interactions occurring to either the carbon or the oxygen atom of the CO. Matrix-isolation experiments validate the expectations of the calculations in revealing the formation of no less than four such isomers when the dihalogen is ICl or IBr, viz. OC \cdots IX, OC \cdots XI, CO \cdots IX, and CO \cdots XI (X = Cl or Br). The complexes have been characterized experimentally by the $\nu(\text{CO})$ bands in their IR spectra, and the $\nu(\text{XY})$ modes of some OC \cdots XY species (XY = Cl₂, BrCl, or ICl) have also been recorded, thereby enabling the perturbation of the acidic component to be assessed.

In purely experimental terms, one of the clearest guides to the strength of the intermolecular interaction is provided by the change in the $\nu(\text{CO})$ wavenumber, $\Delta\nu(\text{CO})$, brought about by complexation. The *blue* shift characterizing complexes of the type OC \cdots XY can be understood in terms of the slight C \cdots O antibonding character of the lone pair orbital localized mainly on the carbon atom of the CO.²⁴ The magnitude of $\Delta\nu(\text{CO})$ (in cm^{-1}), recorded in experiments with Ar matrixes, increases in the order OC \cdots Cl₂ (+2.5) < OC \cdots Br₂ (+5.4)²⁴ < OC \cdots BrI (+7.3/5.0) \leq OC \cdots ClI (+7.4/6.0) < OC \cdots BrCl (+10.2) < OC \cdots IBr (+15.9/12.6) < OC \cdots ICl (+18.8/15.8). The calculated binding energies follow a broadly similar pattern, although they may well underestimate the importance of Coulombic terms, which add appreciably to the stability of the complexes formed by dipolar dihalogens, such as BrCl and ICl. The $\nu(\text{CO})$ shifts may also be compared with those reported for other weak complexes in which CO coordinates through its carbon atom, but to an acidic HX molecule, where X = F,^{8,13} Cl,¹³ Br,¹³ OH,³⁷ or OOH.³⁷ These display $\Delta\nu(\text{CO})$ values ranging from +24 cm^{-1} for OC \cdots HF (in an Ar matrix)⁸ to +9 cm^{-1} for OC \cdots HOH (in an O₂ matrix).³⁷

When CO coordinates through its oxygen atom to an acidic partner, $\nu(\text{CO})$ suffers a *red* shift reflecting the fractional C \cdots O bonding character of the oxygen lone pair. Because this pair lies deeper in energy than the carbon lone pair, CO \cdots XY interactions are significantly weaker than OC \cdots XY interactions, with a much smaller degree of charge transfer (see Table 3) and correspondingly smaller wavenumber shifts, $\Delta\nu(\text{CO})$. On the basis of the present and earlier²⁴ studies of CO \cdots XY species isolated in Ar matrixes, $\Delta\nu(\text{CO})$ (in cm^{-1}) increases in magnitude in the following order: CO \cdots ClI (-1.7) \sim CO \cdots BrI (-1.7) < CO \cdots ClBr (-3.3)²⁴ < CO \cdots Cl₂ (-4.4)²⁴ < CO \cdots Br₂ (-5.5)²⁴ < CO \cdots BrCl (-7.0)²⁴ < CO \cdots IBr (-8.5) < CO \cdots ICl (-9.8). Irrespective of how the CO binds, the heteronuclear dihalogens ICl, IBr, and BrCl emerge as the strongest acids, as long as the more polarizable halogen is the immediate receptor. On the other hand, there is evidence that dipole-dipole interactions make a larger contribution to the stability of CO \cdots XY than to that of their OC \cdots XY isomers. Accordingly, reversal of a heteronuclear dihalogen such as ICl,

IBr, or BrCl so that its dipole is opposed to that of its CO partner results in aggregates of marginal stability and minimal $\Delta\nu(\text{CO})$ values.

The present studies have afforded the first experimental measurements of the $\nu(\text{XY})$ wavenumbers for some complexes of the type OC \cdots XY. Hence, the predicted *red* shift of this mode induced by complexation has been confirmed, with $\Delta\nu(\text{XY})$ values (in cm^{-1}) of -4.1 cm^{-1} for OC \cdots Cl₂, -6.4 cm^{-1} for OC \cdots ICl, and -7.9 cm^{-1} for OC \cdots BrCl. Only in the case of Cl₂ is there a significant body of information regarding its vibrational wavenumber in complexes with different bases. The data reveal $\Delta\nu(\text{Cl}_2)$ values ranging from -7 cm^{-1} for H₂CO \cdots Cl₂ to -85 cm^{-1} for C₂Me₄ \cdots Cl₂.³⁸ CO is a weaker base than any other previously studied in this context, with a proton affinity of 593 kJ mol^{-1} , cf. 718 kJ mol^{-1} for H₂CO.³⁹ The measured $\Delta\nu(\text{Cl}_2)$ of -4.1 cm^{-1} for OC \cdots Cl₂ is therefore consistent with the pattern of earlier results. It need not come as a surprise, however, to find that the correlation between $\Delta\nu(\text{Cl}_2)$ and proton affinity is not particularly close, since Coulombic terms make a relatively minor contribution to the binding of Cl₂ complexes.

Acknowledgment. The authors acknowledge with gratitude a travel grant from the British Council-Fundación Antorchas for British-Argentinian cooperation. R.M.R. thanks Jesus College, Oxford, for financial support and Fundación Antorchas for a grant. In addition, A.J.D. thanks the EPSRC for funding the purchase of equipment.

References and Notes

- (1) Willner, H. Z. *Naturforsch., B: Anorg. Chem., Org. Chem.* **1984**, *39B*, 314.
- (2) Della Védova, C. O.; Mack, H.-G. *Inorg. Chem.* **1993**, *32*, 948.
- (3) Romano, R. M.; Della Védova, C. O.; Downs, A. J.; Greene, T. M. *J. Am. Chem. Soc.* **2001**, *123*, 5794.
- (4) Romano, R. M.; Della Védova, C. O.; Downs, A. J. *J. Phys. Chem. A* **2002**, *106*, 7235.
- (5) Romano, R. M.; Della Védova, C. O.; Downs, A. J. *Chem. Commun.* **2001**, 2638.
- (6) Romano, R. M.; Della Védova, C. O.; Downs, A. J. Unpublished results.
- (7) Thematic issues of *Chem. Rev.* **1988**, *88*, 815-988; **1994**, *94*, 1721-2160; **2000**, *100*, 3861-4264. Bernstein, E. R. *Annu. Rev. Phys. Chem.* **1995**, *46*, 197. Rohrbacher, A.; Halberstadt, N.; Janda, K. C. *Annu. Rev. Phys. Chem.* **2000**, *51*, 405. *Faraday Discuss.* **1994**, *97*, complete issue. *Chem. Phys.* **1998**, *239*, complete issue.
- (8) Schatte, G.; Willner, H.; Hoge, D.; Knözinger, H.; Schrems, O. J. *Phys. Chem.* **1989**, *93*, 6025.
- (9) Legon, A. C.; Soper, P. D.; Keenan, M. R.; Minton, T. K.; Balle, T. J.; Flygare, W. H. *J. Chem. Phys.* **1980**, *73*, 583.
- (10) Legon, A. C.; Soper, P. D.; Flygare, W. H. *J. Chem. Phys.* **1981**, *74*, 4944.
- (11) Kyrö, E. K.; Shoja-Chaghervand, P.; McMillan, K.; Eliades, M.; Danzeiser, D.; Bevan, J. W. *J. Chem. Phys.* **1983**, *79*, 78.
- (12) Fraser, G. T.; Pine, A. S. *J. Chem. Phys.* **1988**, *88*, 4147.
- (13) Andrews, L.; Arlinghaus, R. T.; Johnson, G. L. *J. Chem. Phys.* **1983**, *78*, 6347.
- (14) Andrews, L.; Hunt, R. D. *J. Phys. Chem.* **1988**, *92*, 81.
- (15) Curtis, L. A.; Pochatko, D. J.; Reed, A. E.; Weinhold, F. *J. Chem. Phys.* **1985**, *82*, 2679.
- (16) Bunte, S. W.; Miller, J. B.; Huang, Z. S.; Verdasco, J. E.; Wittig, C.; Beaudet, R. A. *J. Phys. Chem.* **1992**, *96*, 4140.
- (17) Jäger, W.; Xu, Y.; Gary, M. C. L. *J. Phys. Chem.* **1993**, *97*, 3685.
- (18) Hinds, K.; Holloway, J. H.; Legon, A. C. *Chem. Phys. Lett.* **1995**, *242*, 407.
- (19) Waclawik, E. R.; Thumwood, J. M. A.; Lister, D. G.; Fowler, P. W.; Legon, A. C. *Mol. Phys.* **1999**, *97*, 159.
- (20) Blanco, S.; Legon, A. C.; Thorn, J. C. *J. Chem. Soc., Faraday Trans.* **1994**, *90*, 1365.
- (21) Davey, J. B.; Legon, A. C.; Waclawik, E. R. *Phys. Chem. Chem. Phys.* **1999**, *1*, 3097.
- (22) Almond, M. J.; Downs, A. J. *Adv. Spectrosc.* **1989**, *17*, 1. Dunkin, I. R. *Matrix-Isolation Techniques: A Practical Approach*; Oxford University Press: New York, 1998.

- (23) Bunte, S. W.; Chabalowski, C. F.; Wittig, C.; Beaudet, R. A. *J. Phys. Chem.* **1993**, *97*, 5864.
- (24) Schriver, A.; Schriver-Mazzuoli, L.; Chaquin, P.; Bahuo, M. *J. Phys. Chem. A* **1999**, *103*, 2624.
- (25) Matraw, H. C.; Pachucki, C. F.; Hawkins, N. J. *J. Chem. Phys.* **1954**, *22*, 1117.
- (26) Perutz, R. N.; Turner, J. J. *J. Chem. Soc., Faraday Trans. 2* **1973**, *69*, 452.
- (27) Frisch, M. J.; Trucks, G. W.; Schlegel, H. B.; Scuseria, G. E.; Robb, M. A.; Cheeseman, J. R.; Zakrzewski, V. G.; Montgomery, J. A., Jr.; Stratmann, R. E.; Burant, J. C.; Dapprich, S.; Millam, J. M.; Daniels, A. D.; Kudin, K. N.; Strain, M. C.; Farkas, O.; Tomasi, J.; Barone, V.; Cossi, M.; Cammi, R.; Mennucci, B.; Pomelli, C.; Adamo, C.; Clifford, S.; Ochterski, J.; Petersson, G. A.; Ayala, P. Y.; Cui, Q.; Morokuma, K.; Malick, D. K.; Rabuck, A. D.; Raghavachari, K.; Foresman, J. B.; Cioslowski, J.; Ortiz, J. V.; Stefanov, B. B.; Liu, G.; Liashenko, A.; Piskorz, P.; Komaromi, I.; Gomperts, R.; Martin, R. L.; Fox, D. J.; Keith, T.; Al-Laham, M. A.; Peng, C. Y.; Nanayakkara, A.; Gonzalez, C.; Challacombe, M.; Gill, P. M. W.; Johnson, B. G.; Chen, W.; Wong, M. W.; Andres, J. L.; Head-Gordon, M.; Replogle, E. S.; Pople, J. A. *Gaussian 98*, revision A.7; Gaussian, Inc.: Pittsburgh, PA, 1998.
- (28) Wadt, W. R.; Hay, P. J. *J. Chem. Phys.* **1985**, *82*, 284.
- (29) Hay, P. J.; Wadt, W. R. *J. Chem. Phys.* **1985**, *82*, 270.
- (30) Hay, P. J.; Wadt, W. R. *J. Chem. Phys.* **1985**, *82*, 299.
- (31) Nagy, P. I.; Smith, D. A.; Alagona, G.; Ghio, C. *J. Phys. Chem.* **1994**, *98*, 486.
- (32) Boys, S. F.; Benardi, F. *Mol. Phys.* **1970**, *19*, 553.
- (33) Reed, A. E.; Curtiss, L. A.; Weinhold, F. *Chem. Rev.* **1988**, *88*, 889.
- (34) Dubost, H. *Chem. Phys.* **1976**, *12*, 139.
- (35) Ault, B. S.; Howard, W. F., Jr.; Andrews, L. *J. Mol. Spectrosc.* **1975**, *55*, 217.
- (36) Wight, C. A.; Ault, B. S.; Andrews, L. *J. Mol. Spectrosc.* **1975**, *56*, 239. Hawkins, M.; Andrews, L.; Downs, A. J.; Drury, D. J. *J. Am. Chem. Soc.* **1984**, *106*, 3076.
- (37) Tso, T.-L.; Lee, E. K. C. *J. Phys. Chem.* **1985**, *89*, 1612.
- (38) Agarwal, U. P.; Barnes, A. J.; Orville-Thomas, W. J. *Can. J. Chem.* **1985**, *63*, 1705.
- (39) Huheey, J. E.; Keiter, E. A.; Keiter, R. L. *Inorganic Chemistry: Principles of Structure and Reactivity*, 4th ed.; HarperCollins: New York, 1993; pp 318–358.